A self-consistent model for the spiral arms of galaxies

D.J.B.V. Pols

TU Delft
Faculty EEMCS and TNW
BSc Applied Mathematics and Applied Physics
Supervisors: K.W.A. van Dongen and P.M. Visser

25 August 2016
Delft

Abstract

In this thesis, we try to prove the stability of spiral arms using the density wave theory. This theory assumes that the spiral arms are not rigid structures, but instead they are regions with increased density that move through the galaxy like a wave [1]. The spiral structure, in this theory, are driven by the Lindblad resonances, which occur when the star has had an integer amount of radial oscillations for every encounter with the spiral structure. Here, we consider the standard Lindblad model for a two-armed galaxy. We consider the corotation resonance, where the star has the same orbital frequency as the spiral structure, and the Lindblad resonances where the star has completed two radial oscillations for every revolution it has made with respect to the spiral structure. If the star moves more slowly than the spiral structure, it is in the outer Lindblad resonance; if it moves faster than the spiral structure, we call it the inner Lindblad resonance.

To derive a formula for the density of stars in a galaxy, we make a few approximations. We assume that the spiral arms are Archimedian spirals, even though spiral arms are generally shaped more like logarithmic spirals [2]. We also make linear approximations, as we approximate the Hamiltonian in the case without spiral arms with the linear Hamiltonian H_0.

To calculate the density of stars, we assume that the stars follow a certain distribution in phase-space. We then integrate this distribution to obtain the spatial density of the stars. This density shows a clear spiral structure at outer Lindblad resonance and corotation. However, the linear approximations mean that the distribution around inner Lindblad resonance does not show any spiral structure. This is because we linearized the unpertubed Hamiltonian, which means that we assumed that the radial and orbital frequencies are constant for all stars in this resonance. However, when calculating these frequencies using the non-linearized Hamiltonian, we show that this approximation does not work for inner Lindblad resonance, despite being a good assumption for the other resonances. So using this model, we have derived the outer part of the spiral structure. Even though the density in the structure does not differ much from the surrounding galaxy, the increased star formation [3] means that these arms stand out more in luminosity than in density.

Contents

1 Introduction **1**

2 Derivation of the equations of motion for a star **4**
2.1 Dark matter halo 4
2.2 Derivation of the Hamiltonian 4
2.3 Changing to a rotating frame 6

3 Linearization around circular orbits **7**
3.1 Resonances 8
3.2 Exact solution 9

4 Adding a spiral potential **11**

5 Coordinate transformation **12**
5.1 Canonical coordinate transformation 13
5.2 Equations of motion 14
5.3 Transformed Hamiltonian 14
5.4 Time-averaging 15

6 Star distribution **17**

7 Results **19**

8 Discussion and Conclusion **22**

References **23**

Appendix: Code **24**

Nomenclature

Symbol	Description	Physical value for the Milky Way
	Coordinates	
(x, y)	Cartesian coordinates	
r	Radius to the galactic center	
θ	Orbital angle	
θ_{sp}	Orbital angle with respect to the spiral structure	
p	Radial momentum	
l	Angular momentum	
ϕ	Radial phase	
ψ	Orbital phase	
n	Radial amplitude	
t	Time	
	Stellar and galactic properties	
m	Stellar mass	$10^{28} - 10^{32}$ kg [4],[5]
r_+, r_-	Turning points for a star's radial oscillation	
v_0^2	Rotational velocity	~ 210 kpc/Gyr
Ω_s	Angular frequency of the spiral structure	~ 25 rad/Gyr
	Resonance properties	
ω	Orbital frequency in non-rotating frame	
κ	Radial frequency	
a, b	Ratio between κ and $\omega - \Omega_s$	
$\bar{r}$	Radius for a circular orbit in resonance	~ 8.3 kpc for corotation
$\bar{l}$	Angular momentum for a circular orbit in resonance	$m \cdot 1.7$ pc^2/yr for corotation
	Spiral properties	
α	Curve of the spiral arms	~ 0.4 rad/kpc
λ	Disk scale length	~ 0.3 kpc^{-1} [6]
ϵ	Strength of the spiral potential	~ 0.06 [7]
	Energies per unit mass	
$\mathcal{L}$	Lagrangian	
T	Kinetic energy	
V	Potential energy	
V_{sp}	Spiral potential	
$\overline{V}$	Time-averaged spiral potential	
H	Hamiltonian	
H_0	Unpertubed Hamiltonian	
H'	Hamiltonian for the transformed system	
$\overline{H'}$	Time-averaged Hamiltonian	
U	Radial potential	
	Stellar distribution	
f	Distribution in phase-space	
ρ	Spatial density	
β	Energy scale of the distibution	
Z	Normalization constant	

1 Introduction

In this thesis, we consider spiral galaxies. Spiral galaxies, along with irregular galaxies, make up about 60% of the galaxies in the local universe [3]. A few examples of spiral galaxies are Messier 81 and Messier 101, seen in figure 1, where the latter is also known as the Pinwheel galaxy.

(a) Messier 81 [8]

(b) Messier 101, "Pinwheel galaxy" [3]

Figure 1: Examples of spiral galaxies

In both of these galaxies, we can see clear spiral arms extending out from the galactic center. Out of all the galaxies that show a spiral structure, galaxies like Messier 81 and Messier 101 form a minority. About two-thirds of all spiral galaxies also have a bar-shaped structure near the galactic center [9]. Our own galaxy, the Milky Way, belongs to this group. Another example of a spiral galaxy with a central bar is NGC 1300.

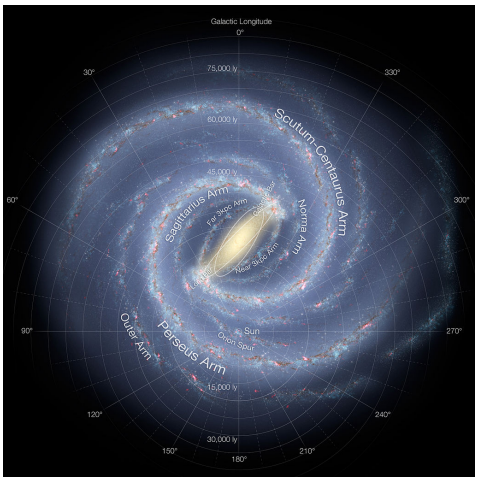

(a) Artist's impression of the Milky Way [10]

(b) NGC 1300 [9]

Figure 2: Some barred spiral galaxies

In the barred spiral galaxies, the spiral arms extend out from the endpoints of the central bar, rather than extending from the galactic center. The model in this thesis works for both regular and barred spiral galaxies.
Since it is not uncommon for galaxies to have a spiral structure, it is worth questioning what caused this structure. Due to the frequent appearance of spiral arms, it is unlikely that they are caused by a purely random event. Originally, astronomers assumed that the spiral arms were rigid mass concentrations. However, it was observed that stars close

to the galactic center have a higher angular frequency than stars that are further away. If the spiral arms are rigid structures, this leads to the "winding problem", where spiral arms become so tightly wound that they are no longer clearly observable [1].
It was proposed that spiral arms instead are "density waves", regions with higher density, that rotate more slowly than the stars in the galaxy [3]. This led to the density wave theory as formulated by C. C. Lin and F. H. Shu [11]. The spiral arms in the density wave theory are driven by Lindblad resonance, which occurs when the star's epicyclic frequency is a multiple of the frequency at which the star encounters the spiral structure.
Galaxies usually have a diameter ranging from 1 kpc to 100 kpc, and can contain between 10^9 to 10^{14} stars [12]. The corotation radius, which is the radius where the stars have the same rotational frequency as the spiral pattern, lies between 7 kpc and 10 kpc [13]. For example, our Sun lies near the corotation radius of the Milky Way [14]. Since the Sun's distance to the galactic center is about 8.3 kpc and the Milky Way is 31-55 kpc in diameter [10], we can see that spiral arms exist at the corotation resonance.

Not in every galaxy are the spiral arm a result of Lindblad resonance. An example of this is the Whirlpool galaxy, NGC 5194, where the spiral arms are believed to result from its interactions with its companion galaxy NGC 5195 [15].

Figure 3: The Whirlpool galaxy and its companion NGC 5195 [15]

The Whirlpool galaxy shows that a collision can induce a spiral structure. This, however, is not always the case. If two spiral galaxies collide, then the resulting galaxy might not have spiral arms. An example of this is the collision of the Milky Way with Andromeda, which is expected to happen in a few billion years. Numerical models of this collision show that the resulting galaxy is an elliptical galaxy [16]. Elliptical galaxies are approximately ellipsoidal in shape, and do not have much structure [17], as we can see from galaxy ESO 325-G004 in figure 4.

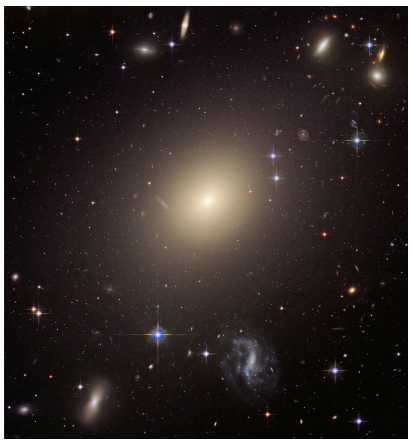

Figure 4: Elliptical galaxy ESO 325-G004 [17]

In this thesis, we do make a few approximations. Most of these approximations are to make the mathematics

simple enough that we can calculate most of the formulas analytically. However, we do also assume that the spiral structure has the shape of an Archimedean spiral.

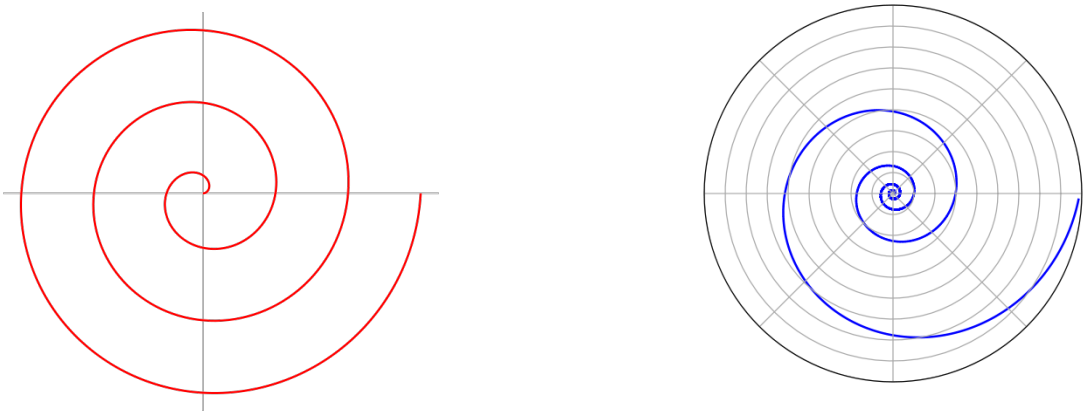

(a) Archimedean spiral

(b) Logarithmic spiral

Figure 5: Two different spirals

The Archimedean spiral has the property that the rotation stays constant, even at a larger radius, meaning that the distance between two consecutive revolutions is constant everywhere. The logarithmic spiral has the property that its shape stays the same, even when scaling it up or down. This does mean that it winds up faster and faster as the radius drops, and is undefined at the origin.
Even though most spiral arms follow the pattern of a logarithmic spiral [2], we assume an Archimedean spiral since we also consider the galactic center in our calculations. Using a logarithmic spiral would mean that some functions are undefined here, which is not a desirable result.

2 Derivation of the equations of motion for a star

The rotation curve or velocity curve of a disc galaxy show the orbital velocity of the galaxy's stars and interstellar gas as a function of the distance to the galactic center. If we would calculate the rotation curves from the visible disc, we would expect the velocity to drop after a certain radius [18]. However, the measured rotation curves are flat, and the expected drop has not been measured yet.

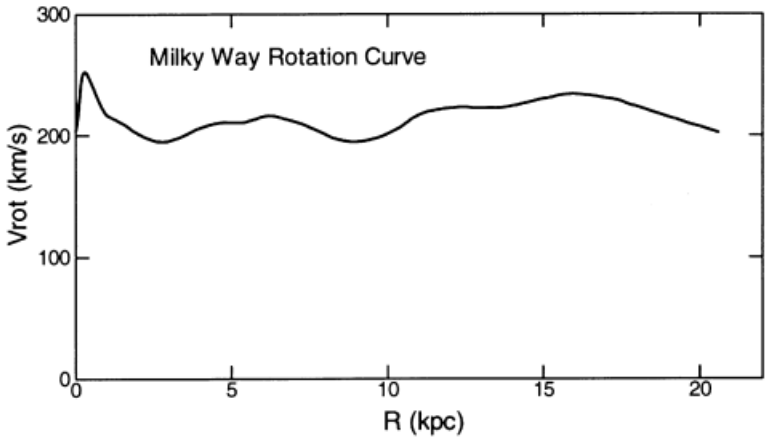

Figure 6: The Milky Way's rotation curve [19].
The velocity does not drop to zero as we would expect from the visible stars and gas

The lack of this expected drop in velocity curves is often explained with a dark matter "halo", a ring of dark matter surrounding the galactic disc.

2.1 Dark matter halo

The velocity curves from figure 6 are evidence of the presence of dark matter. The mass density due to the stars in a galaxy is not enough to produce the potential V, or the rotation curves in figure 6. Assuming that a galaxy has a spherically symmetric mass distribution $\rho = \rho(r)$, then the gravitational force working on a star with distance R from the galactic center, is the same as when all mass inside a sphere with radius R would be concentrated in the galactic center. This galactic force must be the same as the centrifugal force, and since the velocity approaches a constant v_0:

$$\frac{v_0^2}{R} = \frac{GM(R)}{R^2} = \frac{G}{R^2}\int_0^R 4\pi r^2 \rho(r)\ \mathrm{d}r.$$

The mass on a spherical shell with radius r is equal to $4\pi r^2\rho(r)\ \mathrm{d}r$, and summing this mass over all shells from radius 0 to R, gives $M(R)$, the mass inside the sphere with radius R. Now, it follows that the density ρ is proportional to r^{-2}. The galaxy, in approximation, has a uniform stellar mass distribution for $r < r_0$, with r_0 the radius of the galaxy. From this we can conclude that there is another source of mass (dark matter), that gives the total density distribution $\rho(r) \propto r^{-2}$.

2.2 Derivation of the Hamiltonian

The non-relativistic Lagrangian of a system is defined as

$$\mathcal{L} = T - V, \tag{1}$$

where T is the total kinetic energy of the system, and V is the potential energy. If we only consider the motion of one star inside this galaxy, then the kinetic energy is equal to $T = \frac{1}{2}mv^2$. Since m cancels out in the equations of motion, we can replace all energies with energy per unit mass.

Now we want to calculate the velocity v. Note that any velocity can be split into a radial velocity and an angular one. Since the system is a circular disk, we introduce polar coordinates in an inertial frame, so

$$x = r\cos(\theta) \quad \text{and} \quad y = r\sin(\theta).$$

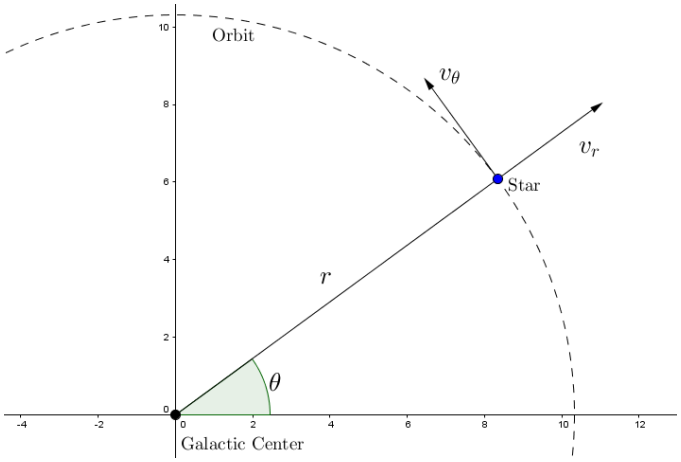

Figure 7: Location and velocities of a star in a galaxy in polar coordinates

The radial velocity v_r is equal to $\dot{r}$, as this velocity is equal to the change in distance to the center. For the angular velocity, first note that $\dot{\theta}$ is the angular frequency (in $\frac{\text{rad}}{s}$). If the star has no radial velocity, it will move in a circular motion, and the time it takes to complete one orbit is $t = \frac{2\pi}{\dot{\theta}}$. Now, the velocity, and therefore the angular velocity is equal to

$$v_\theta = \frac{2\pi r}{t} = \dot{\theta} r,$$

and combining these results gives

$$T = \frac{\dot{r}^2}{2} + \frac{\dot{\theta}^2 r^2}{2}. \tag{2}$$

Since the rotation curves are flat, we know that the velocity of stars approaches a constant v_0 for larger distances to the galactic center as seen in figure 6. The gravitational force is the only force present, so it must be equal to the centrifugal force to keep the stars in orbit, and thus

$$F_z = -\frac{mv^2}{r} = \underbrace{-\frac{v^2}{r}}_{m=1} = \underbrace{-\frac{v_0^2}{r}}_{r \text{ large}}.$$

We know that the force is equal to minus the gradient of the potential,

$$F_z = -\frac{v_0^2}{r} = -\frac{\partial}{\partial r} V,$$

so approximately, we have

$$V = v_0^2 \log(r) + C. \tag{3}$$

Since the constant C does not contibute to the motion of the star, we can set it equal to 0. We do not yet consider a spiral arm in this potential. We call V the dark-matter background potential.
Substituting equations (2) and (3) into (1), we get the Lagrangian

$$\mathcal{L} = \frac{\dot{r}^2}{2} + \frac{\dot{\theta}^2 r^2}{2} - v_0^2 \log(r). \tag{4}$$

From this, we can calculate the conjugate momenta as a function of the velocities:

$$\begin{aligned} p &= \frac{\partial \mathcal{L}}{\partial \dot{r}} = \dot{r} \\ l &= \frac{\partial \mathcal{L}}{\partial \dot{\theta}} = \dot{\theta} r^2. \end{aligned}$$

The Hamiltonian is defined as

$$\begin{aligned} H &= p\dot{r} + l\dot{\theta} - \mathcal{L} \\ &= \frac{p^2}{2} + \frac{l^2}{2r^2} + v_0^2 \log(r). \end{aligned} \tag{5}$$

Here we can see that for this system, the Hamiltonian $H = T + V$, which is the total energy for this star.
From this Hamiltonian, we can calculate the equations of motion using the following system of differential equations

$$\begin{aligned} \dot{r} &= \frac{\partial H}{\partial p} = p \qquad & \dot{p} &= -\frac{\partial H}{\partial r} = \frac{l^2}{r^3} - \frac{v_0^2}{r} \\ \dot{\theta} &= \frac{\partial H}{\partial l} = \frac{l}{r^2} \qquad & \dot{l} &= -\frac{\partial H}{\partial \theta} = 0. \end{aligned} \tag{6}$$

Since we do not yet consider the spiral arms in the potential, the Hamiltonian is axisymmetric, and the angular momentum l is a conserved quantity.

2.3 Changing to a rotating frame

In the previous section, we have found the Hamiltonian in the inertial frame for polar coordinates. However, the properties of the star with respect to the spiral arms are the ones that need to be analyzed. Because of this, it is not useful to calculate the orbit of this star inside the inertial frame, but instead we calculate in a rotating frame. In this frame the spiral arms are stationary.
Assume that the spiral arms rotate with angular frequency Ω_s. Then changing to a rotating frame will add an extra term $-\Omega_s l$ to the Hamiltonian. We can show this in two different ways. First, note that only the θ changes. At any time, the radius and momentum of the star is the same as in the inertial frame, so only the θ is different than before. Since we rotate in the direction of the spiral arms, the angular frequency in the rotating frame is

$$\dot{\theta}_{sp} = \dot{\theta} - \Omega_s.$$

Now note that $\dot{\theta} = \frac{\partial H}{\partial l}$, so to achieve this term $-\Omega_s$, we will need an extra term $-\Omega_s l$ in the Hamiltonian.
Of course, another way to prove this is by using the Lagrangian. We want to change the angle θ to the angle θ_{sp} in the rotating frame. Using the Lagrangian from equation (4)

$$\mathcal{L} = \frac{\dot{r}^2}{2} + \frac{\dot{\theta}^2 r^2}{2} - v_0^2 \log(r),$$

and substituting $\dot{\theta} = \dot{\theta}_{sp} + \Omega_s$, we get

$$\mathcal{L} = \frac{\dot{r}^2}{2} + \frac{(\dot{\theta}_{sp} + \Omega_s)^2 r^2}{2} - v_0^2 \log(r), \tag{7}$$

which gives the conjugate momenta

$$\begin{aligned} p &= \dot{r} \\ l &= (\dot{\theta}_{sp} + \Omega_s) r^2. \end{aligned} \tag{8}$$

Now we get for the Hamiltonian that

$$\begin{aligned} H &= p\dot{r} + l\dot{\theta}_{sp} - \mathcal{L} \\ &= \frac{p^2}{2} + \frac{l^2}{2r^2} + v_0^2 \log(r) - \Omega_s l, \end{aligned} \tag{9}$$

and we get the required term $-\Omega_s l$ in the Hamiltonian.

3 Linearization around circular orbits

It has been observed that stars in a spiral or disk-shaped galaxy move approximately in circular orbits. Consider a star in an exact circular orbit around the galactic center, we know that $r(t) = \bar{r}$ and $\theta(t) = \omega t$, where ω is the angular frequency of this orbit. This also gives that

$$\bar{p} = \dot{r} = 0, \quad \text{and} \quad \bar{l} = \dot{\theta} r^2 = \omega \bar{r}^2.$$

Now assume that the star is not exactly in a circular orbit, but rather near one. This means that $r(t)$ and $\bar{r}$ are not equal, but instead differ by a small value $\delta r(t)$, such that $r(t) = \bar{r} + \delta r(t)$. Similarly, $\theta(t) = \omega t + \delta\theta(t)$, $p = \bar{p} + \delta p$ and $l = \bar{l} + \delta l$. Substituting this into the Hamiltonian from equation (9), we get

$$\begin{aligned} H &= \frac{p^2}{2} + \frac{l^2}{2r^2} - \Omega_s l + v_0^2 \log(r) \\ &= \frac{(\bar{p} + \delta p)^2}{2} + \frac{(\bar{l} + \delta l)^2}{2(\bar{r} + \delta r)^2} - \Omega_s(\bar{l} + \delta l) + v_0^2 \log(\bar{r} + \delta r). \end{aligned}$$

Since the unknowns $(\delta r, \delta\theta, \delta p, \delta l)$ are small, we can expand the Hamiltonian to the second order around the circular orbit with $\delta r, \delta\theta, \delta p, \delta l = 0$.

$$\begin{aligned} H = \frac{\bar{p}^2}{2} + \frac{\bar{l}^2}{2\bar{r}} - \Omega_s \bar{l} + v_0^2 \log(\bar{r}) + \delta r \left[-\frac{\bar{l}^2}{\bar{r}^3} + \frac{v_0^2}{\bar{r}} \right] + (\delta p)\bar{p} + \delta l \left[\frac{\bar{l}}{\bar{r}^2} - \Omega_s \right] + (\delta l)^2 \frac{1}{2\bar{r}^2} \\ + (\delta r)^2 \left[\frac{3}{2} \frac{\bar{l}^2}{\bar{r}^4} - \frac{v_0^2}{2\bar{r}^2} \right] + (\delta l)(\delta r) \left[-\frac{\bar{l}}{\bar{r}^3} \right] + \frac{(\delta p)^2}{2}. \end{aligned} \tag{10}$$

Extracting the equations of motion out of the expanded Hamiltonian in equation (10), we get

$$\begin{aligned} \delta\dot{r} &= \frac{\partial H}{\partial \delta p} = \bar{p} + \delta p = \delta p \\ \omega + \delta\dot{\theta} &= \frac{\partial H}{\partial \delta l} = \frac{\bar{l}}{\bar{r}^2} - \Omega_s + \frac{\delta l}{\bar{r}^2} - \delta r \frac{\bar{l}}{\bar{r}^3} \\ \delta\dot{p} &= -\frac{\partial H}{\partial \delta r} = \frac{\bar{l}^2}{\bar{r}^3} - \frac{v_0^2}{\bar{r}} - \delta r \left[3\frac{\bar{l}^2}{\bar{r}^4} - \frac{v_0^2}{\bar{r}^2} \right] + \delta l \frac{\bar{l}}{\bar{r}^3} \\ \delta\dot{l} &= -\frac{\partial H}{\partial \delta\theta} = 0. \end{aligned}$$

Since the circular orbit is a stationary point for the Hamiltonian (a star in a circular orbit stays in that orbit), we expect the Hamiltonian to approach a harmonic oscillator around this point. Therefore, if we take $(\delta r, \delta\theta, \delta p, \delta l)$ small enough, we are left with just constants and second order terms. This means that all linear terms should vanish, and thus

$$\begin{cases} \frac{v_0^2}{\bar{r}} - \frac{\bar{l}^2}{\bar{r}^3} = 0 \\ \frac{\bar{l}}{\bar{r}^2} - \Omega_s = 0 \end{cases}$$

so $\bar{l} = v_0 \bar{r}$ and $\bar{l} = \Omega_s \bar{r}^2$, from which it follows that $v_0 = \Omega_s \bar{r}$, and $\Omega_s = \omega$.
This yields a linear system of differential equations, where we use that $\bar{l} = \omega \bar{r}^2$

$$\begin{aligned} \delta\dot{r} &= \delta p \\ \Omega_s + \delta\dot{\theta} &= \frac{\delta l}{\bar{r}^2} - \delta r \frac{\omega}{\bar{r}} \\ \delta\dot{p} &= -2\delta r \omega^2 + \delta l \frac{\omega}{\bar{r}} \\ \delta\dot{l} &= 0. \end{aligned}$$

and in the inertial frame (where the Ω_s vanishes), we can rewrite this to

$$\begin{pmatrix} \delta\dot{r} \\ \delta\dot{\theta} \\ \delta\dot{p} \\ \delta\dot{l} \end{pmatrix} = \begin{pmatrix} 0 & 0 & 1 & 0 \\ -\frac{\omega}{\bar{r}} & 0 & 0 & \frac{1}{\bar{r}^2} \\ -2\omega^2 & 0 & 0 & \frac{\omega}{\bar{r}} \\ 0 & 0 & 0 & 0 \end{pmatrix} \begin{pmatrix} \delta r \\ \delta\theta \\ \delta p \\ \delta l \end{pmatrix} \tag{11}$$

which has eigenvalues $\lambda = 0$ (with a multiplicity of 2), $\lambda = \pm i\sqrt{2}\omega = \pm i\sqrt{2}\frac{v_0}{\bar{r}}$. All non-zero eigenvalues are purely imaginary, meaning that the stationary solutions of this system are stable. If the star has an orbit close to a stationary solution, so its orbit is almost circular, the orbit will stay near this circular orbit.
Since the general solution of this linearized system has the form

$$e^{\lambda t}\mathbf{v},$$

where $\mathbf{v}$ is an eigenvector of matrix (11), we can see that the system has an epicyclic frequency

$$\kappa = \sqrt{2}\frac{v_0}{\bar{r}}. \tag{12}$$

Since the orbit had an angular frequency $\omega = \frac{v_0}{\bar{r}}$, the epicyclic frequency is also $\kappa = \sqrt{2}\omega$.

If we do not require the linear term in l to become zero, and instead ignore the quadratic term, then

$$\left(\frac{\bar{l}}{\bar{r}^2} - \Omega_s\right)\delta l = (\omega - \Omega_s)\delta l.$$

Using the epicyclic frequency κ in equation (12), the quadratic term in r becomes

$$\left(\frac{2\bar{l}^2}{3\bar{r}^4} - \frac{v_0^2}{2\bar{r}^2}\right)\delta r^2 = \frac{\kappa^2}{2}\delta r^2.$$

If we also drop the constants, the linearized Hamiltonian becomes

$$H_0(r, \theta, p, l) = \frac{p^2}{2} + \frac{\kappa^2}{2}(r - \bar{r})^2 + (\omega - \Omega_s)l. \tag{13}$$

The motions of stars in nearly circular orbits should be well approximated by H_0.

3.1 Resonances

Resonances occur when an integer number of epicyclic oscillations coincide with an integer number of orbits, so in the rotating frame,

$$a(\omega - \Omega_s) = b\kappa, \tag{14}$$

with $a, b \in \mathbb{Z}$. We can assume that $a > 0$. Considering only $2:1$ resonances, this model has $a = 2$ and $b = \pm 1$ or $b = 0$, where $b = 1$ for inner Lindblad resonance, and $b = -1$ for outer Lindblad resonance. If $b = 0$, then $\omega = \Omega_s$, and the star is in corotation with the spiral arms.
From $2(\omega - \Omega_s) = \pm\kappa$ and $\kappa = \sqrt{2}\omega$, it follows that

$$\omega = \frac{\sqrt{2}}{\sqrt{2} \mp 1}\Omega_s \qquad \kappa = \frac{2}{\sqrt{2} \mp 1}\Omega_s, \tag{15}$$

with the minus sign for inner Lindblad resonance, and the plus sign for outer Lindblad resonance. Furthermore, the equilibrium radius and angular momentum of this orbit, when expressed in Ω_s and v_0, become

$$\bar{r} = \left(1 \mp \frac{1}{\sqrt{2}}\right)\frac{v_0}{\Omega_s} \qquad \bar{l} = \left(1 \mp \frac{1}{\sqrt{2}}\right)\frac{v_0^2}{\Omega_s}. \tag{16}$$

The Lindblad resonances are the closed orbits in the rotating frame where the spiral arms are stationary. If the orbits are not closed, then the effects of the spiral arms will reach their maximum at a different phase on every orbit, so the total change will average to zero. For the closed orbits, these effects will occur at the same phase every orbit, so the change adds up and does not nullify itself. This is why we consider only the Lindblad resonances and corotation.

3.2 Exact solution

If we do not consider spiral arms, then the system is axisymmetric with respect to the galactic center. This means that the angular momentum l is conserved in this system. This follows from the Hamiltonian (9), which is independent of θ. Also note that this Hamiltonian is time-independent, so it represents a constant of motion, and it is also conserved. So we have $l = L$ and $H = E$ for this system. Now, the motion of the star in this two-dimensional plane is integrable. We can write the radial velocity as

$$\dot{r} = p = \pm\sqrt{2E - \frac{L^2}{r^2} + 2\Omega_s L - 2v_0^2 \log(r)}.$$

We define

$$U(r) = \frac{L^2}{2r^2} - \Omega_s L + v_0^2 \log(r)$$

as the radial potential.

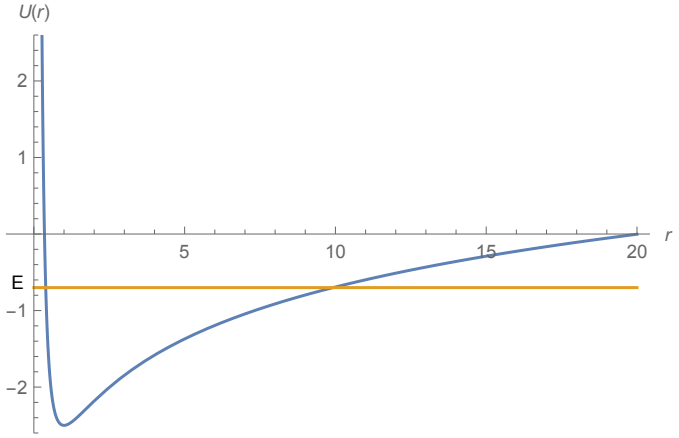

Figure 8: The radial potential energy versus r. A star with energy E moves radially between the two turning points r_- and r_+ where $U(r)$ is equal to E

From Figure 8, we can see that there are two radii for which $U(r) = E$, and thus $p = 0$. Therefore the radial motion is bound between these two turning points, so $r_- \leq r \leq r_+$. For these points, we have

$$E = \frac{L^2}{2r_-^2} - \Omega_s L + v_0^2 \log(r_-) = \frac{L^2}{2r_+^2} - \Omega_s L + v_0^2 \log(r_+).$$

From this, we can calculate the angular momentum as a function of the turning points

$$L = v_0 r_- r_+ \sqrt{\frac{2}{r_+^2 - r_-^2} \log\left(\frac{r_+}{r_-}\right)}.$$

Substituting this back, we find an expression for the energy

$$E = v_0^2 \frac{r_+^2 \log(r_+) - r_-^2 \log(r_-)}{r_+^2 - r_-^2} - \Omega_s L.$$

Since the time it takes to travel between the turning points is half the radial oscillation time, we get for the frequencies

$$\frac{\pi}{\kappa} = \int_0^{\pi/\kappa} \mathrm{d}t = \int_{r_-}^{r_+} \frac{\mathrm{d}r}{p} \qquad \text{and} \qquad \frac{\omega\pi}{\kappa} = \int_{r_-}^{r_+} \frac{\dot{\theta} + \Omega_s}{\dot{r}}\, \mathrm{d}r = \int_{r_-}^{r_+} \frac{L}{r^2 p}\, \mathrm{d}r.$$

Using the expressions for p, E and L, this becomes

$$\frac{\pi}{\kappa} = \frac{\sqrt{r_+^2 - r_-^2}}{v_0\sqrt{2}} \int_{r_-}^{r_+} \left(r_+^2 \log\left(\frac{r_+}{r}\right) + r_-^2 \log\left(\frac{r}{r_-}\right) - \frac{r_-^2 r_+^2}{r^2} \log\left(\frac{r_+}{r_-}\right) \right)^{-\frac{1}{2}} \mathrm{d}r \tag{17}$$

and

$$\frac{\omega\pi}{\kappa} = r_+ r_- \sqrt{\log\left(\frac{r_+}{r_-}\right)} \int_{r_-}^{r_+} \left(r_+^2 \log\left(\frac{r_+}{r}\right) + r_-^2 \log\left(\frac{r}{r_-}\right) - \frac{r_-^2 r_+^2}{r^2} \log\left(\frac{r_+}{r_-}\right) \right)^{-\frac{1}{2}} \frac{\mathrm{d}r}{r^2}. \tag{18}$$

For a certain resonance, we need

$$\frac{\omega - \Omega_s}{\kappa} = \frac{\omega}{\kappa} - \frac{\Omega_s}{\kappa} = \frac{b}{a}$$

to hold. Using equations (17) and (18), we can find the turning points for different resonances, and calculate the corresponding frequencies κ and ω. These frequencies are plotted in figure 9.

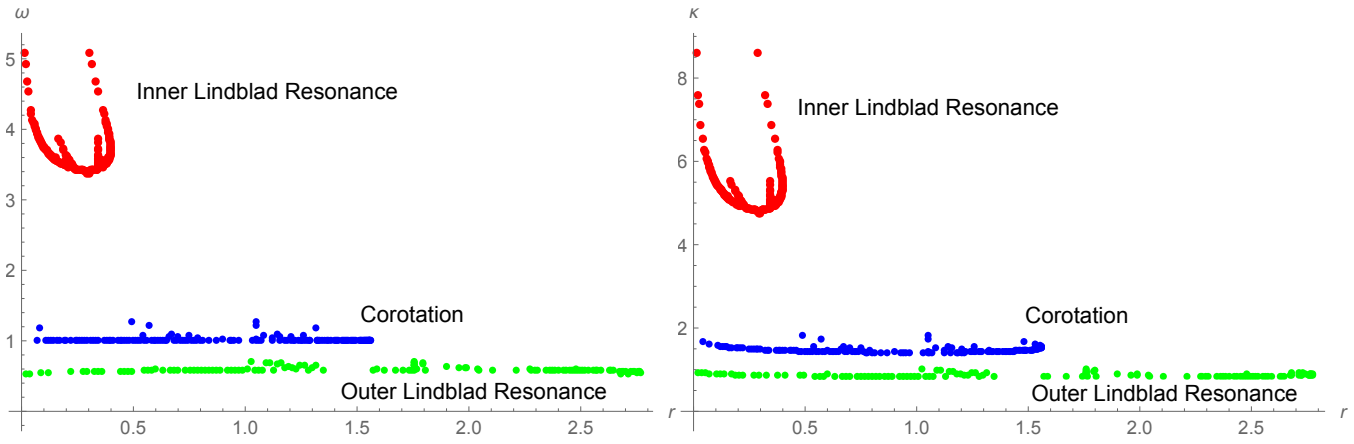

(a) ω at resonance

(b) κ at resonance

Figure 9: The angular and radial frequencies, ω and κ respectively, at resonance for different turning points. The data is calculated using equations (17) and (18)

We can see that the frequencies ω and κ stay constant over a wide range of amplitudes at corotation and outer Lindblad resonance, but that at inner Lindblad resonance, they increase quickly when the amplitude becomes larger.

4 Adding a spiral potential

If we want to add a spiral potential to the Hamiltonian, we must go back to the Lagrangian. The kinetic energy in the rotating frame has not changed, so

$$\mathcal{L} = \frac{\dot{r}^2}{2} + \frac{(\dot{\theta}_{sp} + \Omega_s)^2 r^2}{2} - V.$$

Since we want to add a potential due to the spiral arms, the potential energy V is no longer equal to $v_0^2 \log(r)$ as it was in equation (7). Here,

$$V = v_0^2 \log(r) + V_{sp},$$

where V_{sp} is the potential caused by the spiral structure. In the rotating frame, the spiral arms are stationary and give an extra potential with the form of an Archimedian spiral

$$V_{sp} = \varepsilon e^{-\lambda r} \cos(\alpha r - 2\theta). \tag{19}$$

Here, ε is the strenght of the potential, and is only a small number, as the spiral arms only have a slight effect on the motion of the star. λ makes the potential approach zero for larger radii, and α indicates the curve of the spiral arms.

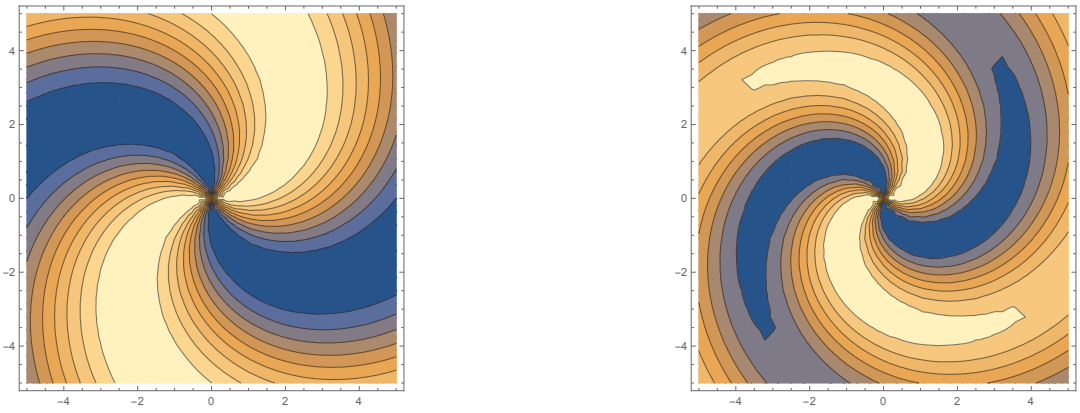

(a) Spiral potential with $\alpha = 0.5$, $\lambda = 0$

(b) Spiral potential with $\alpha = 1$, $\lambda = 0.1$

Figure 10: Examples of the spiral potential for different α and λ

Now note that the spiral potential V_{sp} does not depend on the velocities $\dot{r}$ and $\dot{\theta}$. Because of this, the formulas for the conjugate momenta p and l do not differ from the ones we got in equation (8), which means that for the Hamiltonian, we get

$$H = \frac{p^2}{2} + \frac{l^2}{2r^2} - \Omega_s l + v_0^2 \log(r) + \varepsilon e^{-\lambda r} \cos(\alpha r - 2\theta).$$

Using this Hamiltonian, we can calculate the motion of the stars, where we now do consider the spiral arms. The system of differential equations that we use to calculate this motion becomes

$$\begin{aligned} \dot{r} &= \frac{\partial H}{\partial p} = p & \dot{p} &= -\frac{\partial H}{\partial r} = \frac{l^2}{r^3} - \frac{v_0^2}{r} - \frac{\partial V_{sp}}{\partial r} \\ \dot{\theta} &= \frac{\partial H}{\partial l} = \frac{l}{r^2} - \Omega_s & \dot{l} &= -\frac{\partial H}{\partial \theta} = -\frac{\partial V_{sp}}{\partial \theta}. \end{aligned} \tag{20}$$

Since we now have a spiral potential, the Hamiltonian is no longer rotationally symmetric, and the angular momentum l is not constant.

5 Coordinate transformation

We are not interested in the general solution of the Hamilton equations. Instead, we want to research the deviation between the true orbits and the solutions from the unpertubed Hamiltonian H_0 from (13). To do so, we now transform this problem from polar coordinates (r, θ, p, l) to the variables (ϕ, ψ, n, l) that change slowly in time. If we take a reference point that has a circular orbit of radius $\bar{r}$ around the galactic center, and let this point move with constant orbital frequency $\omega - \Omega_s$, then ψ is the difference between the orbital angle of the star and that of this reference point. The radial oscillation of the star around $r = \bar{r}$ has amplitude proportional to $\sqrt{n}$, and phase $\phi + \kappa t$. The new angular momentum l is the same as the old one.

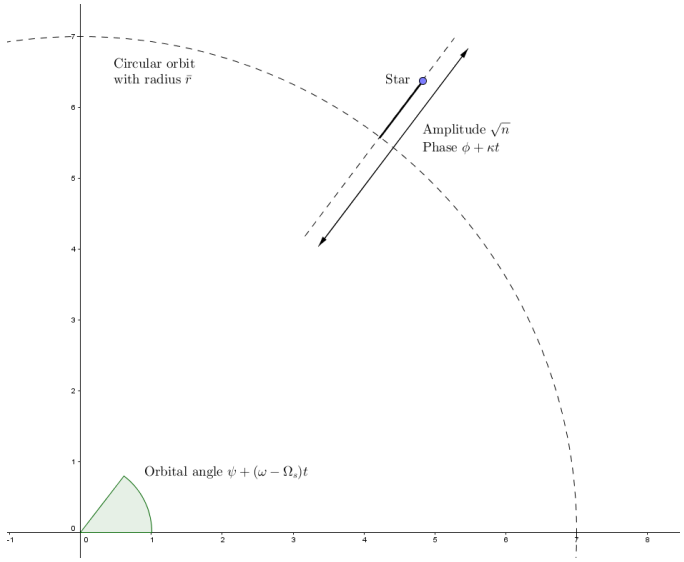

Figure 11: The slow variables

This is summarized in the coordinate transformation

$$\begin{cases} r = \bar{r} + \sqrt{\dfrac{2n}{\kappa}} \cos(\phi + \kappa t) \\ p = \quad -\sqrt{2n\kappa} \sin(\phi + \kappa t) \\ \theta = \psi + (\omega - \Omega_s)t \\ l = l \end{cases} \tag{21}$$

with inverse transformation

$$\begin{cases} \phi = \arctan\left(-\dfrac{p}{\kappa(r - \bar{r})}\right) - \kappa t \\ n = \dfrac{\kappa}{2}(r - \bar{r})^2 + \dfrac{p^2}{2\kappa} \\ \psi = \theta - (\omega - \Omega_s)t \\ l = l. \end{cases} \tag{22}$$

Note that for constant ϕ, ψ, n, l, the functions (21) are exactly the solutions of the system defined by the Hamiltonian H_0 given by (13).
The transformation from (r, p) to (ϕ, n) is like a harmonic oscillator transformation. [20, Chapter 9]
A simple harmonic oscillator has the Hamiltonian

$$H = \frac{1}{2m}(p^2 + m^2\omega^2 q^2).$$

Now, using the transformation

$$q = \sqrt{\frac{2P}{m\omega}}\sin(Q)$$
$$p = \sqrt{2Pm\omega}\cos(Q),$$

the Hamiltonian becomes $H = \omega P$.

In the same way, the transformation (21) takes the quadratic part of the linearized Hamiltonian (13), $\frac{p^2}{2} + \frac{\kappa^2}{2}(r-\bar{r})$ and transforms it into a linear term. Therefore, this Hamiltonian in the new variables becomes

$$H_0 = \kappa n + (\omega - \Omega_s)l. \tag{23}$$

5.1 Canonical coordinate transformation

To calculate the new Hamiltonian in the new coordinates, we first must show that this transformation is canonical. A canonical transformation is a coordinate transformation that preserves the form of Hamilton's equations (the equations of motion). When transforming from coordinates (r, θ) and conjugate momenta (p, l) to the new coordinates (ϕ, ψ) and corresponding momenta (n, l), then the transformation is canonical if it satisfies the direct conditions [21]

$$\frac{\partial(\phi,\psi)}{\partial(p,l)} = -\frac{\partial(r,\theta)}{\partial(n,l)}, \qquad \frac{\partial(\phi,\psi)}{\partial(r,\theta)} = \frac{\partial(p,l)}{\partial(n,l)}$$
$$\frac{\partial(n,l)}{\partial(r,\theta)} = -\frac{\partial(p,l)}{\partial(\phi,\psi)}, \qquad \frac{\partial(n,l)}{\partial(p,l)} = \frac{\partial(r,\theta)}{\partial(\phi,\psi)}.$$

For example, this means that $\frac{\partial\phi}{\partial r} = \frac{\partial p}{\partial n}$, or that $\frac{\partial n}{\partial\theta} = -\frac{\partial p}{\partial\psi}$. Most of the direct conditions give trivial results, as these equations give zero, like $\frac{\partial r}{\partial\psi}$ or $\frac{\partial\theta}{\partial n}$, or 1, like $\frac{\partial l}{\partial l}$. Four of the direct conditions are not trivial. The transformation can be shown to obey these conditions using that

$$\cos(\arctan(x)) = \frac{1}{\sqrt{x^2+1}}, \qquad \sin(\arctan(x)) = \frac{x}{\sqrt{x^2+1}},$$

for all $x \in \mathbb{R}$. For example, with the direct condition $\frac{\partial\phi}{\partial p} = -\frac{\partial r}{\partial n}$,

$$\begin{aligned}
\frac{\partial\phi}{\partial p} &= \frac{\partial}{\partial p}\left[\arctan\left(-\frac{p}{\kappa(r-\bar{r})}\right) - \kappa t\right] \\
&= -\frac{1}{\kappa(r-\bar{r})}\left(\frac{p^2}{\kappa^2(r-\bar{r})^2}+1\right)^{-1} \qquad \text{since } \frac{\partial}{\partial x}\arctan(x) = \frac{1}{x^2+1} \\
&= -\frac{\kappa(r-\bar{r})}{p^2+\kappa^2(r-\bar{r})^2}.
\end{aligned}$$

Also,

$$\begin{aligned}
-\frac{\partial r}{\partial n} &= -\sqrt{\frac{1}{2n\kappa}}\cos(\phi+\kappa t) \\
&= -\sqrt{\frac{1}{\kappa^2(r-\bar{r})^2+p^2}}\cos\left(\arctan\left(-\frac{p}{\kappa(r-\bar{r})}\right)\right) \\
&= -\sqrt{\frac{1}{\kappa^2(r-\bar{r})^2+p^2}}\frac{\kappa(r-\bar{r})}{\sqrt{p^2+\kappa^2(r-\bar{r})^2}} \\
&= -\frac{\kappa(r-\bar{r})}{p^2+\kappa^2(r-\bar{r})^2}.
\end{aligned}$$

So indeed, $\frac{\partial\phi}{\partial p} = -\frac{\partial r}{\partial n}$. The conditions

$$\frac{\partial\phi}{\partial r} = \frac{\partial p}{\partial n}, \qquad \frac{\partial n}{\partial p} = \frac{\partial r}{\partial\phi}, \qquad \frac{\partial n}{\partial r} = -\frac{\partial p}{\partial\phi}$$

can be proven in the same way as the one above.

5.2 Equations of motion

We can obtain the new equations of motion directly from the transformation equations. Since l remains unchanged by this transformation, we get

$$\dot{l} = -\frac{\partial V_{sp}[r(\phi,n),\theta(\psi),p(\phi,n),l]}{\partial\theta}.$$

The transformation rule for θ only depends on ψ, and

$$\dot{\psi} = \dot{\theta} - (\omega - \Omega_s) = \frac{l}{\left(\bar{r} + \sqrt{\frac{2n}{\kappa}}\cos(\phi+\kappa t)\right)^2} - \omega.$$

For the radial coordinates ϕ and n, the transformation can be compactly written as

$$(r-\bar{r}) + i\frac{p}{\kappa} = \sqrt{\frac{2n}{\kappa}}e^{-i(\phi+\kappa t)}.$$

Taking the time derivative, this becomes

$$\dot{r} + i\frac{\dot{p}}{\kappa} = \left(\frac{\dot{n}}{2n} - i(\dot{\phi}+\kappa)\right)\sqrt{\frac{2n}{\kappa}}e^{-i(\phi+\kappa t)}$$
$$\frac{\dot{n}}{2n} - i(\dot{\phi}+\kappa) = \left(\dot{r} + i\frac{\dot{p}}{\kappa}\right)\sqrt{\frac{\kappa}{2n}}e^{i(\phi+\kappa t)}.$$

Since the real and imaginary parts of these equations have to be the same, we can conclude that

$$\dot{n} = \sqrt{2n\kappa}\left(\dot{r}\cos(\phi+\kappa t) - \frac{\dot{p}}{\kappa}\sin(\phi+\kappa t)\right)$$
$$\dot{\phi} = -\sqrt{\frac{\kappa}{2n}}\left(\dot{r}\sin(\phi+\kappa t) + \frac{\dot{p}}{\kappa}\cos(\phi+\kappa t)\right) - \kappa.$$

Substituting $\dot{r}$ and $\dot{p}$ with their equations of motion (20) and transforming to the new variables, we obtain:

$$\dot{n} = -2n\kappa\cos(\phi+\kappa t)\sin(\phi+\kappa t) - \sqrt{\frac{2n}{\kappa}}\dot{p}\sin(\phi+\kappa t)$$
$$\dot{\phi} = \kappa\sin^2(\phi+\kappa t) - \sqrt{\frac{1}{2n\kappa}}\dot{p}\cos(\phi+\kappa t) - \kappa,$$

where for $\dot{p}$ we must substitute

$$\dot{p} = \frac{l^2}{r(\phi,n)^3} - \frac{v_0^2}{r(\phi,n)} - \frac{\partial V_{sp}[r(\phi,n),\theta(\psi),p(\phi,n),l]}{\partial r}.$$

5.3 Transformed Hamiltonian

Since the transformation from (r,θ,p,l) to (ϕ,ψ,n,l) is canonical, the new equations of motion are also Hamilton equations. The equations of motion for $\phi(t),\psi(t),n(t),l(t)$ are controlled by a new Hamiltonian, which is the difference between the old Hamiltonian and the unpertubed Hamiltonian H_0 [20, Chapter 12]:

$$H' = H - H_0.$$

In the new coordinates, this Hamiltonian is equal to

$$\begin{aligned} H' &= \frac{p^2}{2} + \frac{l^2}{2r^2} + v_0^2\log(r) - \Omega_s l + V_{sp}(r,\theta,p,l) - H_0 \\ &= \kappa n\sin^2(\phi+\kappa t) + \frac{l^2}{2\left[\bar{r} + \sqrt{\frac{2n}{\kappa}}\cos(\phi+\kappa t)\right]^2} + v_0^2\log\left(\bar{r} + \sqrt{\frac{2n}{\kappa}}\cos(\phi+\kappa t)\right) \\ &+ V_{sp}(\phi,\psi,n,l) - (\kappa n + \omega l)\,. \end{aligned}$$

In these coordinates, the Hamilton equations are

$$\dot{\phi} = \frac{\partial H'}{\partial n}, \qquad \dot{\psi} = \frac{\partial H'}{\partial l}, \qquad \dot{n} = -\frac{\partial H'}{\partial \psi}, \qquad \dot{l} = -\frac{\partial H'}{\partial \psi}.$$

Since

$$V_{sp}(\phi, \psi, n, l) = \varepsilon e^{-\lambda r(\phi,n)} \cos(\alpha r(\phi, n) - 2\psi - 2(\omega - \Omega_s)t),$$

the Hamilton equations are identical to the equations of motion calculated from the transformation (21). Since H' is the correct Hamiltonian for the slow variables, this independently confirms that the transformation (21) is canonical.

5.4 Time-averaging

In the unpertubed system where the stars' orbits are driven by the zero-Hamiltonian H_0, the stars move with angular frequency $\omega - \Omega_s$, and have radial frequency κ. Since stars move approximately in circular orbits, and circular orbits give constant ϕ, ψ, n, l, the slow variables that define these orbits change slowly or stay constant in time. The change in these variables over one orbit is small, we can instead consider the secular change over many orbits, which is give by the time-averaged Hamiltonian [20]. The method of slow variables used in this model is devised by Visser.
The stars approximately have angular frequency $\omega - \Omega_s$, so the time it takes to complete one orbit is equal to

$$t = \frac{2\pi}{\omega - \Omega_s}.$$

Therefore, the time-averaged Hamiltonian must be defined as

$$\overline{H'} = \frac{\omega - \Omega_s}{2\pi} \int_0^{2\pi/(\omega-\Omega_s)} H' \, \mathrm{d}t.$$

Note that

$$\frac{\omega - \Omega_s}{2\pi} \int_0^{2\pi/(\omega-\Omega_s)} \frac{1}{1 + \sqrt{\frac{\kappa n}{v_0^2}} \cos(\phi + \kappa t)} \mathrm{d}t = \left(1 - \frac{\kappa n}{v_0^2}\right)^{3/2}.$$

We can calculate

$$\frac{\omega - \Omega_s}{2\pi} \int_0^{2\pi/(\omega-\Omega_s)} \log\left(1 + \sqrt{\frac{\kappa n}{v_0^2}} \cos(\phi + \kappa t)\right) \mathrm{d}t$$

by time-averaging the derivative with respect to n of this logarithm, and integrating the resulting function. This yields

$$\frac{\omega - \Omega_s}{2\pi} \int_0^{2\pi/(\omega-\Omega_s)} \log\left(1 + \sqrt{\frac{\kappa n}{v_0^2}} \cos(\phi + \kappa t)\right) \mathrm{d}t = \log\left(1 + \sqrt{1 - \frac{\kappa n}{v_0^2}}\right).$$

Combining this result with $\frac{2n}{\kappa \bar{r}^2} = \frac{\kappa n}{v_0^2}$, we obtain for the time-averaged Hamiltonian

$$\overline{H'} = \frac{\kappa^2 l^2}{4v_0^2 \left(1 - \frac{\kappa n}{v_0^2}\right)^{3/2}} + v_0^2 \log\left(1 + \sqrt{1 - \frac{\kappa n}{v_0^2}}\right) - \frac{\kappa n}{2} - \omega l + \overline{V}, \tag{24}$$

where $\overline{V}$ is the time-averaged spiral potential.
In the old variables, the spiral potential is equal to

$$V(r, \theta, p, l) = \varepsilon e^{-\lambda r} \cos(\alpha r - 2\theta).$$

Using $\cos(x) = \mathrm{Re}(e^{ix})$, this can be rewritten to

$$V(r, \theta, p, l) = \varepsilon \, \mathrm{Re}\left[e^{i(\alpha + i\lambda)r - 2i\theta}\right].$$

Substituting the new variables, this becomes

$$V(\phi, \psi, n, l) = \varepsilon \, \mathrm{Re}\left[e^{i(\alpha+i\lambda)\bar{r}} e^{i(\alpha+i\lambda)\sqrt{\frac{2n}{\kappa}}\cos(\phi+\kappa t)} e^{-2i\psi} e^{-ib\kappa t}\right].$$

Now we can use the Fourier series

$$e^{iz\cos(x)} = \sum_{h=-\infty}^{\infty} i^h J_h(z) e^{ihx},$$

where J_h are the Bessel functions of the first kind, to write the spiral potential as

$$V(\phi, \psi, n, l) = \varepsilon \ \mathrm{Re}\left[\sum_{h=-\infty}^{\infty} e^{i(\alpha+i\lambda)\bar{r}} J_h\left((\alpha+i\lambda)\sqrt{\frac{2n}{\kappa}}\right) e^{i(h\phi-2\psi)} e^{i(h-b)\kappa t}\right].$$

When averaging over the orbital period, and thus over an integer amount of radial oscillations, all term vanish except for the constant term where $h = b$. This gives that

$$\overline{V}(\phi, \psi, n, l) = \varepsilon \ \mathrm{Re}\left[e^{i(\alpha+i\lambda)\bar{r}} J_b\left((\alpha+i\lambda)\sqrt{\frac{2n}{\kappa}}\right) e^{i(b\phi-2\psi)}\right]. \tag{25}$$

6 Star distribution

We want to calculate the way the stars distribute themselves inside the galaxy due to the spiral potential. For this, we assume that there is a time-independent distribution of stars $f(\phi, \psi, n, l)$ in the slow variables. Using the coordinate rules (21), we can transform this to a distribution in the original coordinates using

$$f(r, \theta, p, l) = \iiint \overline{\delta\left(r - r(t)\right) \delta\left(\theta - \theta(t)\right) \delta\left(p - p(t)\right)} f(\phi, \psi, n, l) \ \mathrm{d}\phi \ \mathrm{d}\psi \ \mathrm{d}n,$$

where the overline again represents the time-averaged function. Hence $f(r, \theta, p, l)$ is a time-independent function. With this distribution, we can calculate the spatial density of stars ρ inside the galaxy by integrating over the conjugate momenta:

$$\rho(r, \theta) = \frac{1}{r} \iint f(r, \theta, p, l) \ \mathrm{d}p \ \mathrm{d}l.$$

The $\frac{1}{r}$ term is the Jacobian that occurs when transforming from cartesian coordinates to polar coordinates. Now, if the distribution f is normalized, then the density ρ will be normalized as well. Now note that the expression for the density has become

$$\rho(r, \theta) = \frac{1}{r} \iint \iiint \overline{\delta\left(r - r(t)\right) \delta\left(\theta - \theta(t)\right) \delta\left(p - p(t)\right)} f(\phi, \psi, n, l) \ \mathrm{d}\phi \ \mathrm{d}\psi \ \mathrm{d}n \ \ \mathrm{d}p \ \mathrm{d}l.$$

The coordinate p is independent from ϕ, ψ, n, l, and

$$\int_{-\infty}^{\infty} \delta\left(p - p(t)\right) \ \mathrm{d}p = 1,$$

so we have

$$\rho(r, \theta) = \frac{1}{r} \iiint \overline{\delta\left(r - r(t)\right) \delta\left(\theta - \theta(t)\right)} \int f(\phi, \psi, n, l) \ \mathrm{d}l \ \ \mathrm{d}\phi \ \mathrm{d}\psi \ \mathrm{d}n.$$

Here, we have to integrate ϕ and ψ from 0 to 2π, and l from $-\infty$ to ∞. The boundaries for the n-integral will prove to be at $n = \frac{\kappa}{2}(r - \bar{r})^2$ and $n = \frac{\kappa \bar{r}^2}{2}$.

To obtain the spatial density of stars, $\rho(r, \theta)$, we have to make an assumption on the initial distribution f. Since the stable resonances are found at the minima of $\overline{H'}$, we assume a distribution like a maximal-entropy state:

$$f(\phi, \psi, n, l) = \frac{1}{Z} e^{-\beta \overline{H'}(\phi, \psi, n, l)},$$

where Z is a normalization constant. Due to this maximal-entropy state, the stars are most likely to find themselves in the stable orbits near the minima of $\overline{H'}$. Because of this, it is reasonable to assume this state as the initial distribution. Simultaneously, this state is the Laplace transform of $\delta(E - \overline{H'})$, so even if this state is not the correct initial distribution, it is still useful to calculate the density due to this state. The method for calculating the density of stars is devised by Visser, who also proposed this initial star distribution.

First, let us evaluate the integral over l.

$$\int_{-\infty}^{\infty} \exp\left(\beta \omega L - \beta \frac{\kappa^2 l^2}{4 v_0^2 \left(1 - \frac{\kappa n}{v_0^2}\right)}\right) \ \mathrm{d}l.$$

Since

$$\int_{-\infty}^{\infty} \exp\left(-Al^2 - Bl\right) \ \mathrm{d}l = \sqrt{\frac{\pi}{A}} e^{\frac{B^2}{4A}} \quad \text{if } \mathrm{Re}(A) > 0,$$

this integral becomes equal to

$$\sqrt{\frac{2\pi}{\beta}} \bar{r} \left(1 - \frac{\kappa n}{v_0^2}\right)^{3/4} \ \exp\left(\frac{1}{2} \beta \omega^2 \bar{r}^2 \left[1 - \frac{\kappa n}{v_0^2}\right]^{3/2}\right).$$

Now we need to evaluate the integrals over ϕ and ψ. In the Hamiltonian $\overline{H'}$, only $\overline{V}$ depends on these variables, so these integrals only affect this term.

$$\iint \overline{\delta\left(r - r(t)\right)\delta\left(\theta - \theta(t)\right)} e^{-\beta\overline{V}(\phi,\psi,n,l)}\,\mathrm{d}\phi\,\mathrm{d}\psi.$$

Since $\psi = \theta - (\omega - \Omega)t = \frac{b}{a}\kappa t$, where $a = 2$ and $b = -1, 0, 1$, we can rewrite this to

$$\int \overline{\delta\left(r - r(t)\right) e^{-\beta\overline{V}(\phi,\theta-\frac{b}{2}\kappa t,n,l)}}\,\mathrm{d}\phi.$$

This becomes

$$\overline{e^{-\beta\overline{V}}} = \frac{\kappa}{\sqrt{2\kappa n - \kappa^2(r-\bar{r})^2}}\left(e^{-\beta\overline{V}(\phi_1(r,n),\theta,n)} + e^{-\beta\overline{V}(\phi_2(r,n),\theta,n)}\right),$$

where

$$\phi_1(r,n) = -\arccos\left((r-\bar{r})\sqrt{\frac{\kappa}{2n}}\right) \quad \text{and} \quad \phi_2(r,n) = \arccos\left((r-\bar{r})\sqrt{\frac{\kappa}{2n}}\right).$$

Since the star density has to be real, the root in the denominator of $\overline{e^{-\beta\overline{V}}}$,

$$\sqrt{2\kappa n - \kappa^2(r-\bar{r})^2},$$

must be real. Therefore, there are only contributions from

$$\frac{\kappa}{2}(r-\bar{r})^2 < n < \frac{\kappa\bar{r}^2}{2}.$$

These conditions can be rewritten to

$$(r-\bar{r}) < \sqrt{\frac{2n}{\kappa}} < \bar{r}.$$

This means that we only get contributions if the amplitude of the radial oscillation around $\bar{r}$ is large enough that we can actually reach a point at radius r, but not so large that the radius could become smaller than zero. This also implies that r has to be smaller than $2\bar{r}$.
Also note that

$$\exp\left(-\beta v_0^2 \log\left(1 + \sqrt{1 - \frac{\kappa n}{v_0^2}}\right)\right) = \left(1 + \sqrt{1 - \kappa n / v_0^2}\right)^{-\beta v_0^2}$$

and

$$\frac{\kappa n}{2} = \frac{1}{2}\omega^2\bar{r}^2\frac{\kappa n}{v_0^2}.$$

Now we can express the star density ρ as a single integral over n:

$$\rho(r,\theta) = \sqrt{\frac{2\pi}{\beta}}\frac{\bar{r}}{Zr}\int_{\frac{\kappa}{2}(r-\bar{r})^2}^{\frac{\kappa\bar{r}^2}{2}} \left(1 - \frac{\kappa n}{v_0^2}\right)^{3/4} e^{\frac{1}{2}\beta\omega^2\bar{r}^2\left[\left(1-\frac{\kappa n}{v_0^2}\right)^{3/2} + \frac{\kappa n}{v_0^2}\right]} \left(1 + \sqrt{1 - \frac{\kappa n}{v_0^2}}\right)^{-\beta v_0^2} \overline{e^{-\beta\overline{V}}}\,\mathrm{d}n. \tag{26}$$

We can use this equation (26) to calculate the density of stars around $\bar{r}$ for a specific resonance.

7 Results

Equation (26) still contains $\bar{r}$ and b, both of which depend on the resonance we consider. Because of this, we can only show the density of the stars around one of the Lindblad resonances. The extra density inside the spiral arms is a small amount compared to the density in the galaxy, so the spiral structure is visualized the best using contour plots. Here we use 200 contour levels. At all resonances, the contours are strictly increasing when approaching the galactic center, except at small radii.

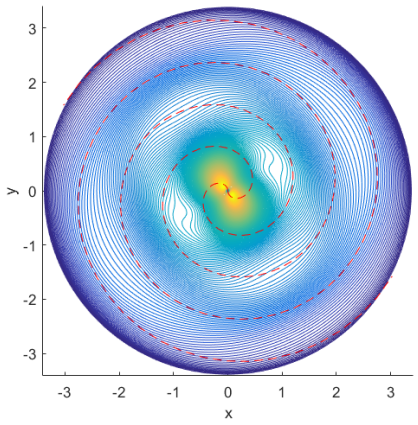

(a) $\alpha = 4$, $\lambda = .2$, $\beta = 4$, $\varepsilon = .3$

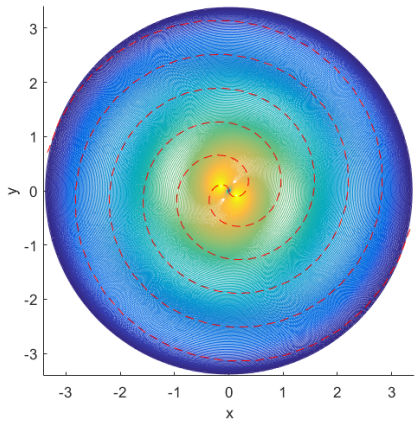

(b) $\alpha = 5$, $\lambda = .5$, $\beta = 2.5$, $\varepsilon = .3$

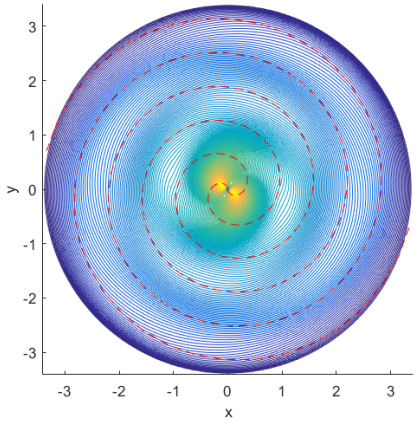

(c) $\alpha = 5$, $\lambda = .7$, $\beta = 3.5$, $\varepsilon = .5$

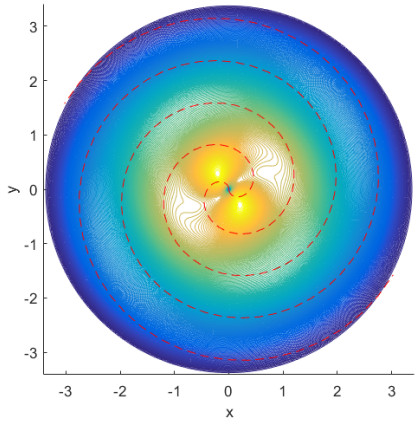

(d) $\alpha = 4$, $\lambda = .3$, $\beta = 1.5$, $\varepsilon = .5$

Figure 12: Density of stars near outer Lindblad resonance;
the dashed red line indicates the assumed spiral arms

The density of stars shows an central elliptical orbit due to the resonance, from which a faint arm spirals outward, and an arm spirals inward. For lower values of β, the outward-spiralling arm becomes less visible as the difference in density between it and the surrounding part of the galaxy becomes smaller. This is to be expected, as lower values of β, so $\beta \approx 0$, give an axisymmetric result for the density of stars. In contrast, higher values for β push the stars not only into the orbits with maximum amplitude, but also along the angular minima of the spiral potential.

We can also calculate the density of stars for orbits near corotation.

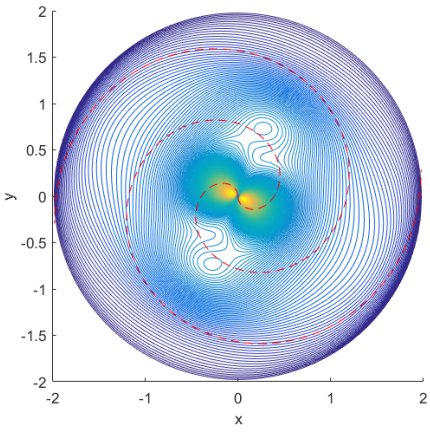

(a) $\alpha = 4$, $\lambda = .2$, $\beta = 4$, $\varepsilon = .3$

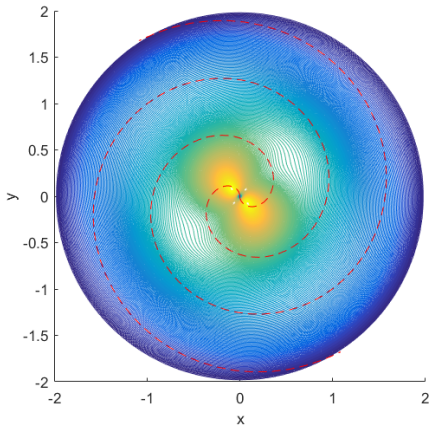

(b) $\alpha = 5$, $\lambda = .5$, $\beta = 2.5$, $\varepsilon = .3$

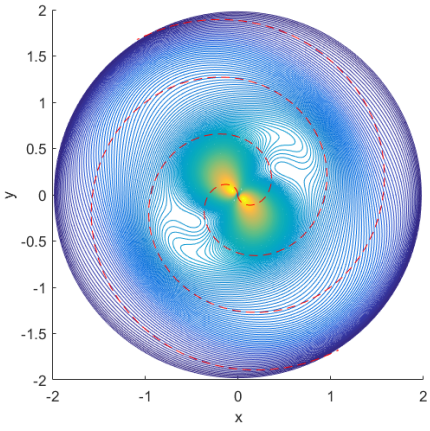

(c) $\alpha = 5$, $\lambda = .7$, $\beta = 3.5$, $\varepsilon = .5$

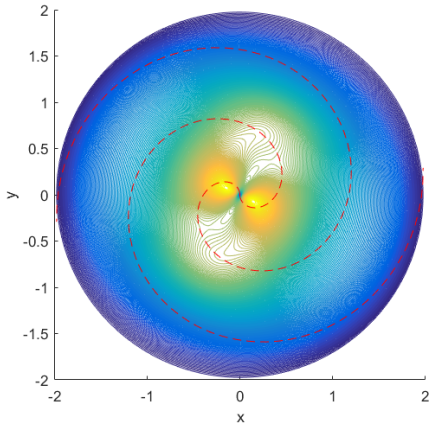

(d) $\alpha = 4$, $\lambda = .3$, $\beta = 1.5$, $\varepsilon = .5$

Figure 13: Density of stars near corotation;
the dashed red line indicates the assumed spiral arms

Apart from the maximum density near the galactic center, we see two bulges in the density that are aligned with the spiral potential. Since the stars in corotation are stationary with respect to the spiral arms, the stars will clump together near the minima of the spiral arms. When β increases, again the stars will be forced into orbits with higher eccentricity, but the term $\overline{e^{-\beta\overline{V}}}$ will push the stars toward these bulges at the corotation resonance.

Again, we use equation (26) to calculate the density of stars at inner Lindblad resonance.

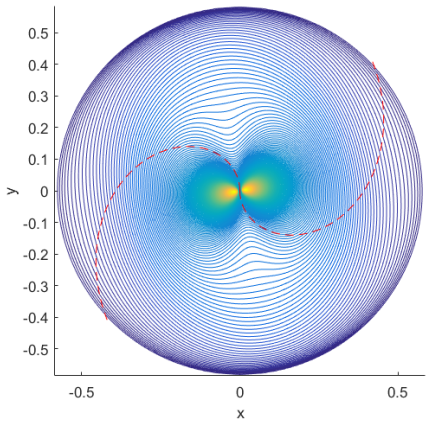

(a) $\alpha = 4$, $\lambda = .2$, $\beta = 4$, $\varepsilon = .3$

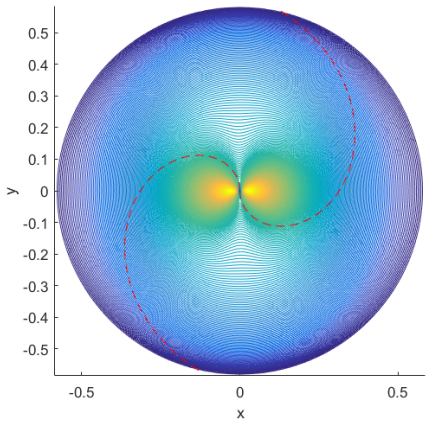

(b) $\alpha = 5$, $\lambda = .5$, $\beta = 2.5$, $\varepsilon = .3$

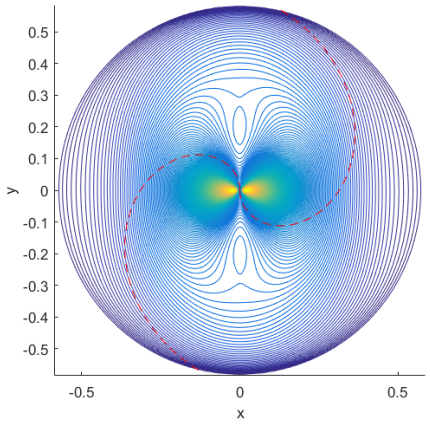

(c) $\alpha = 5$, $\lambda = .7$, $\beta = 3.5$, $\varepsilon = .5$

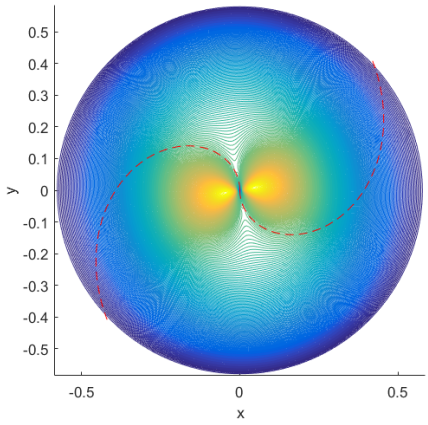

(d) $\alpha = 4$, $\lambda = .3$, $\beta = 1.5$, $\varepsilon = .5$

Figure 14: Density of stars near inner Lindblad resonance;
the dashed red line indicates the assumed spiral arms

At inner Lindblad resonance, the density of stars is devoid of any spiral structure. If we were to consider only the spiral potential, the stars would move in orbits with maximum amplitude that do not follow the spiral potential.

8 Discussion and Conclusion

From figures 12 to 14, we can see that the results give no spiral structure near the inner Lindblad resonance. This is unfortunate, as the inner Lindblad resonance should contribute the most towards the total spiral structure. Because the amount of stars decreases for larger radii, most of the stars will follow the inner resonance.
The problem with our approximations for inner Lindblad resonance lies in equation (13). Because we chose H_0 to be linear in l, we assume that ω, and therefore also κ, are independent of the radius of the orbit of the star, and are only influenced by the resonance that the star follows. After calculating the frequencies as a function of the turning points in figure 9, we can see that at the inner Lindblad resonance, κ and ω change quickly when approaching higher amplitudes. This problem is nonexistent for corotation and outer Lindblad resonance, as in these resonances, the frequencies stay nearly constant over the entire range of amplitudes.

A way to combat this is to consider higher order terms in the linearized Hamiltonian (13). If, for example, we do not stop after the linear term in l, and instead include the quadratic term in l and the term $(r-\bar{r})(l-\bar{l})$, the motion in θ will become nontrivial. After transforming the Hamiltonian, we need to linearize the transformed H_0 in n and l, to make sure that the frequencies do not depend on the slow coordinates. If they do, then the secular approximation will fail since we cannot calculate the time-average. After all, it is impossible to calculate the coordinates from the time-averaged system, if the time period over which we average depends on the coordinates.

In figures 12 and 13, we can see that the results give a spiral structure near outer Lindblad resonance and corotation. For galaxies like the Milky Way, spiral arms still exist at corotation and outer Lindblad resonance. Since the corotation radius is approximately 8 kpc, outer Lindblad resonance exists around 13 kpc, as $\bar{r}$ for the outer resonance is around 1.7 times larger than the corotation radius. The radius of the Milky Way is between 15 to 25 kpc, so the outer Lindblad resonance is still relevant. This means that using this model, we have found a spiral structure in the density of stars that could resemble the outer part of the spiral arms for these galaxies. Even though the added density is small, this does mean that the spiral arms are regions of increased star formation [3]. Because of this, even though the relative change in density is small, the spiral arms are a lot brighter, as these regions contain more young, bright stars.

We should note that when calculating the density at the outer Lindblad resonance, that there is also an arm spiralling inwards that appears to spiral in the opposite direction compared to the assumed spiral arms. This result is not detrimental to the validity of this model, as spiral galaxies usually have arms that split up. In this case, one arm splits into two, where one spirals outward and the other spirals inward, which is what we see in figure 12.

Now, we have shown that an initial spiral potential V_{sp} leads to a spiral structure in the density of stars. Since the derived structure follows the assumed spiral potential, we can say that the spiral arms are self-consistent. After all, a spiral arm superimposes a faint spiral potential onto the existing background potential. However, the spiral potential does not have to be created by stars. If, for example, the distribution of interstellar gas or dark matter contained a spiral structure, this would also have led to the formation of spiral arms.

References

[1] "Density wave theory." https://en.wikipedia.org/wiki/Density_wave_theory. Version 29 May 2016 18:24.

[2] G. Bertin and C. C. Lin, *Spiral Structure in Galaxies: A Density Wave Theory*. The MIT Press, first edition ed., 1996.

[3] "Spiral galaxy." https://en.wikipedia.org/wiki/Spiral_galaxy. Version 28 May 2016 13:53.

[4] "List of brown dwarfs." https://en.wikipedia.org/wiki/List_of_brown_dwarfs. Version 26 July 2016 05:45.

[5] "List of most massive stars." https://en.wikipedia.org/wiki/List_of_most_massive_stars. Version 22 July 2016 18:15.

[6] J. Bovy and H.-W. Rix, "A Direct Dynamical Measurement of the Milky Way's Disk Surface Density Profile, Disk Scale Length, and Dark Matter Profile at 4 kpc $\lesssim$ R $\lesssim$ 9 kpc," *Astrophysical Journal*, vol. 779, p. 115, Dec. 2013.

[7] C. A. Martínez-Barbosa, A. G. A. Brown, and S. Portegies Zwart, "Radial migration of the Sun in the Milky Way: a statistical study," *Monthly Notices of the Royal Astronomical Society*, vol. 446, pp. 823–841, Jan. 2015.

[8] "Messier 81." https://en.wikipedia.org/wiki/Messier_81. Version 29 March 2016 22:36.

[9] "Barred spiral galaxy." https://en.wikipedia.org/wiki/Barred_spiral_galaxy. Version 24 July 2016 14:29.

[10] "Milky way." https://en.wikipedia.org/wiki/Milky_Way. Version 20 July 2016 17:41.

[11] C. C. Lin and F. H. Shu, "On the Spiral Structure of Disk Galaxies," *Astrophysical Journal*, vol. 140, pp. 646–655, Aug. 1964.

[12] "Galaxy." https://en.wikipedia.org/wiki/Galaxy. Version 11 August 2016 21:12.

[13] W. S. Dias and J. R. D. Lépine, "Direct determination of the spiral pattern rotation speed of the galaxy," *Astrophysical Journal*, vol. 625, pp. 825–831, Aug. 2005.

[14] Y. N. Mishurov and I. A. Zenina, "Yes, the Sun is located near the corotation circle," *Astronomy and Astrophysics*, vol. 341, pp. 81–85, Jan. 1999.

[15] "Whirlpool galaxy." https://en.wikipedia.org/wiki/Whirlpool_Galaxy. Version 19 July 2016 12:24.

[16] "Andromeda-milky way collision." https://en.wikipedia.org/wiki/Andromeda-Milky_Way_collision. Version 21 July 2016 09:10.

[17] "Elliptical galaxy." https://en.wikipedia.org/wiki/Elliptical_galaxy. Version 25 May 2016 03:03.

[18] "Galaxy rotation curve." https://en.wikipedia.org/wiki/Galaxy_rotation_curve. Version 31 July 2016 02:44.

[19] Y. Sofue, Y. Tutui, M. Honma, A. Tomita, T. Takamiya, J. Koda, and Y. Takeda, "Central rotation curves of spiral galaxies," *The Astrophysical Journal*, vol. 523, pp. 136–146, Sept. 1999.

[20] H. Goldstein, C. P. Poole, and J. L. Safko, *Classical mechanics*. Addison-Wesley, third edition ed., 2001.

[21] "Canonical transformation." https://en.wikipedia.org/wiki/Canonical_transformation. Version 5 August 2015 17:04.

[22] MATLAB 9.0 (R2016a), The MathWorks Inc., Natick, MA, 2016.

[23] Wolfram Research, Inc., Mathematica, Version 11.0, Champaign, IL (2016).

Appendix: Code

These are the MATLAB [22] scripts used to generate figures 12 to 14. The main code saves the constants for the function `rho` to load.

```
function y=rho(r,theta,h,l) %defining the density
load('constants.mat')       %loading the constants from the other file
omega = 1/(1-sqrt(2)*h/l)*Omega;
kappa = sqrt(2)*omega;
rbar = v0/omega;

if((r/rbar -1)^2+0.01<0.99) %If we can create an x (where x = kappa*n/v0^2)
    x = linspace((r/rbar -1)^2+0.01,0.99,100); %create a range of x to integrate over
                                               %so that the Inf at the
                                               %boundaries are avoided

    V = @(n) eps.*real(1i^h.*besselj(h,(alpha+1i.*lambda).*sqrt(2.*x).*v0./kappa)...
        .*exp(1i.*(alpha+1i*lambda).*rbar-2.*1i.*theta)...
        .*exp((-1)^n.*h.*1i.*acos((r-rbar)./(rbar.*sqrt(x)))));

    bV = 1./sqrt(rbar^2.*x-(r-rbar)^2).*(...
        exp(-b.*V(1))+exp(-b.*V(2))); %Define e^{-beta*V}

    %The total function we integrate over
    f = (1-x).^(3/4).*(1+sqrt(1-x)).^(-b*v0^2).*exp(0.5*b*omega^2*rbar^2.*((1-x).^(3/2)+x)).*bV;

    y=trapz(x,f)/r; %Integrate over x and divide by r.
                    %The constants are not important as only the shape
                    %matters
else
    y=0; %If we are out of range, there are no stars.
end
```

```
clear;clc;
%% Define constants
tic;
v0 = 1;
Omega = 1;
alpha = 4;
lambda = .3;
eps = .5;
b = 3.5;

h=-1;
l=2;
omega = 1/(1-sqrt(2)*h/l)*Omega;
kappa = sqrt(2)*omega;
rbar = v0/omega;
lbar = v0*rbar;

scale = 2*rbar;
res = 200;
x = linspace(-scale,scale,res);
y = linspace(-scale,scale,res);

data = zeros(res);
save('constants','v0','Omega','alpha','lambda','eps','b'); %save constants for rho
%%
parfor i = 1:length(x) %parallel processing
    temp1 = zeros(1,length(y));
    for j = 1:length(y)
        [theta,r]=cart2pol(x(i),y(j));%(x,y) to (r,theta) for rho to use
        temp1(j)=rho(r,theta,h,l); %Calculate rho for all x,y
    end
```

```
    data(i,:)=temp1;
end

r = linspace(0,2*rbar,100);
t1 = alpha.*r-pi/2;
t2 = alpha.*r+pi/2;
[a,b] = pol2cart(t1,r);
[a2,b2]=pol2cart(t2,r);%The minima of the spiral potential
%%
databw = data/max(max(data));%databw has a maximum of 1 to be used by imshow
[X,Y]=meshgrid(x,y);
figure;
hold on
contour(X,Y,data,200)%create a contour plot of rho
xlabel('x')
ylabel('y')
axis equal tight
line(a,b,max(max(data))*ones(size(a)),'color','r','LineStyle','--');
line(a2,b2,max(max(data))*ones(size(a)),'color','r','LineStyle','--');
hold off
figure;
imshow(flip(databw,2))
toc;
```

This is the Mathematica [23] script used to generate figure 9.

```
Omega = 1; (*Defining the constants*)
v0 = 1;
h = 1;
l = 2;
rbar = (1 - Sqrt[2] * h / l) v0 / Omega;
res = 100;
(*Defining relevant functions*)
tau[a_, b_] := Sqrt[b^2 - a^2] / (v0 * Sqrt[2]) * NIntegrate[1 / (Sqrt[b^2 Log[b / r] + a^2 Log[r / a] - a^2 b^2 / r^2 Log[b / a]]), {r, a, b}];
sigma[a_, b_] := b a Sqrt[Log[b / a]] * NIntegrate[1 / (Sqrt[b^2 Log[b / r] + a^2 Log[r / a] - a^2 b^2 / r^2 Log[b / a]]) / r^2, {r, a, b}];
hoverl[a_, b_] := sigma[a, b] / Pi - Omega * tau[a, b] / Pi;
kappa[a_, b_] := Pi / tau[a, b];
omega[a_, b_] := sigma[a, b] / tau[a, b];
(*Calculating the lower and upper turning points*)
rm = Table[0 + i * rbar / res, {i, 1, res}];
rp = Table[Re[x] /. FindRoot[hoverl[rm[[i]], x] == h / l, {x, rbar + 0.05}, Evaluated → False], {i, 1, res}]; // Quiet
lowerlist1 = Table[{rm[[i]], kappa[rm[[i]], rp[[i]]]}, {i, 1, Length[rm]}];
upperlist1 = Table[{rp[[i]], kappa[rm[[i]], rp[[i]]]}, {i, 1, Length[rm]}];
(*The same for corotation*)
h = 0;
rbar = (1 - Sqrt[2] * h / l) v0 / Omega;
rm = Table[0 + i * rbar / res, {i, 1, res}];
rp = Table[Re[x] /. FindRoot[hoverl[rm[[i]], x] == h / l, {x, rbar + 0.05}, Evaluated → False], {i, 1, res}]; // Quiet
lowerlist2 = Table[{rm[[i]], kappa[rm[[i]], rp[[i]]]}, {i, 1, Length[rm]}];
upperlist2 = Table[{rp[[i]], kappa[rm[[i]], rp[[i]]]}, {i, 1, Length[rm]}];
(*The same for outer Lindblad resonance*)
h = -1;
rbar = (1 - Sqrt[2] * h / l) v0 / Omega;
rm = Table[0 + i * rbar / res, {i, 1, res}];
rp = Table[Re[x] /. FindRoot[hoverl[rm[[i]], x] == h / l, {x, rbar + 0.05}, Evaluated → False], {i, 1, res}]; // Quiet
(*Outputting the figures*)
lowerlist3 = Table[{rm[[i]], kappa[rm[[i]], rp[[i]]]}, {i, 1, Length[rm]}];
upperlist3 = Table[{rp[[i]], kappa[rm[[i]], rp[[i]]]}, {i, 1, Length[rm]}];
upper1 = ListPlot[upperlist1, PlotStyle → Red];
lower1 = ListPlot[lowerlist1, PlotStyle → Red];
upper2 = ListPlot[upperlist2, PlotStyle → Blue];
lower2 = ListPlot[lowerlist2, PlotStyle → Blue];
upper3 = ListPlot[upperlist3, PlotStyle → Green];
lower3 = ListPlot[lowerlist3, PlotStyle → Green];
Show[lower1, upper1, lower2, upper2, lower3, upper3, PlotRange → All , AxesOrigin → {0, 0},
 AxesLabel -> {ToExpression["r", TeXForm, HoldForm], ToExpression["\\kappa", TeXForm, HoldForm]}]
```